

# Periodically Fully Developed Flow in Channels with Conducting Blockages

S. H. Kim\* and N. K. Anand†

Texas A&M University, College Station, Texas 77843

The numerical treatment of periodically fully developed flow in channels with conducting blockages is presented. The significance of the second source term  $\partial(K\sigma)/\partial x$  is illustrated in the energy equation by studying heat transfer in a two-dimensional rectangular channel with surface-mounted blocks on the bottom wall. The SIMPLER algorithm was employed to solve the periodically fully developed channel problem. The periodically developed flow solution and the developing flow solution from the channel entrance were compared. Calculations were made for different values of  $Re$ ,  $K$ , and geometric parameters. It is found that the inclusion of the second source term results in the prediction of the correct temperature field. In general, any parameter that would increase  $\partial(K\sigma)/\partial x$  will strengthen the second source term effect.

## Nomenclature

$B$	= channel height
$C_p$	= specific heat at constant pressure
$d$	= exit length
$J$	= flux
$K$	= ratio of $k_s$ to $k_f$
$k_f$	= fluid thermal conductivity
$k_s$	= solid thermal conductivity
$L$	= length of the channel
$\ell$	= length of the module
$P$	= pressure or block length
$q''$	= heat flux
$Re$	= Reynolds number ( $Re = \rho \bar{u} B / \mu$ )
$S$	= source term or spacing
$T$	= temperature
$T_b$	= bulk temperature ( $T_b = \int_0^B u T dy / \int_0^B u dy$ )
$u$	= velocity in $x$ direction
$v$	= velocity in $y$ direction
$x, y$	= coordinates
$\beta$	= global pressure drop
$\Gamma$	= transport coefficient
$\mu$	= dynamic viscosity
$\rho$	= density of the fluid
$\sigma$	= global temperature rise
$\phi$	= field variable
$\Psi$	= stream function

## Subscripts

0	= channel entrance
$s$	= streamwise direction
$w$	= wall
$x$	= axial direction
min	= minimum

## Superscripts

$\wedge$	= periodic fluctuation
$-$	= average value

## Introduction

THE hydrodynamic and thermal boundary layers of flows in channels with periodic variations in flow cross sections

are periodically interrupted. The periodic interruption of boundary layers will result in periodically fully developed flow. The geometry of the channel repeats itself from module to module; consequently, heat transfer and fluid flow will also repeat itself from module to module. The periodic variation of flow area in channels may be the result of the periodic variation of the shape of the channel wall or may be due to the presence of periodic blockages in the flow path.

Patankar et al.<sup>1</sup> developed and discussed the theory of "periodically fully developed flow" in channels and its numerical implementation. Even though the theory and development were comprehensive, no special attention was given to channels with conducting blockages. Patankar and Prakash<sup>2</sup> studied laminar heat transfer in periodically interrupted plate passages. Attention was given to the effect of plate thickness on heat transfer and fluid flow. A very high value of thermal conductivity was assigned to the solid to achieve uniform wall temperature conditions. Other investigators<sup>3,4</sup> extended the concepts of Patankar et al.<sup>1</sup> to study periodically fully developed flow and heat transfer in channels with conducting blockages.

The objective of this paper is to develop a procedure to treat periodically fully developed heat-transfer problems in channels with conducting blockages. The treatment of momentum field remains the same as discussed in Patankar et al.<sup>1</sup> The numerical implementation is illustrated via a contrived example problem.

## Procedure

In this work, consideration is given to steady-state, two-dimensional, incompressible elliptic flow in a channel with periodically varying cross-sectional area. The periodic variation in flow cross section is due to the presence of conducting blockages such as ribs, fins, heated blocks, and so forth. In general terms, the two-dimensional conservation equation with a source term is

$$\frac{\partial J_x}{\partial x} + \frac{\partial J_y}{\partial y} = S \quad (1)$$

where

$$J_x = \rho u \phi - \Gamma \frac{\partial \phi}{\partial x} \quad \text{and} \quad J_y = \rho v \phi - \Gamma \frac{\partial \phi}{\partial y} \quad (2)$$

In the above equation,  $\phi$  is a general field variable and  $\Gamma$  is the transport coefficient. Our focus in this work is the temperature field. The discussion of Patankar et al.<sup>1</sup> follows:

$$\phi = \sigma x + \hat{\phi} \quad (3)$$

Received July 23, 1990; revision received Jan. 10, 1991; accepted for publication Jan. 15, 1991. Copyright © 1991 by the American Institute of Aeronautics and Astronautics, Inc. All rights reserved.

\*Graduate Research Assistant, Department of Mechanical Engineering.

†Associate Professor, Department of Mechanical Engineering.

where  $\sigma$  is the global temperature rise per module and  $\hat{\phi}$  is the local temperature rise. Substituting Eqs. (2) and (3) into Eq. (1) and rearranging the equation we get

$$\frac{\partial}{\partial x} \left[ \rho u \hat{\phi} - \Gamma \frac{\partial \hat{\phi}}{\partial x} \right] + \frac{\partial}{\partial y} \left[ \rho v \hat{\phi} - \Gamma \frac{\partial \hat{\phi}}{\partial y} \right] + \sigma x \left[ \frac{\partial \rho u}{\partial x} + \frac{\partial \rho v}{\partial y} \right] = S - \rho u \sigma + \frac{\partial}{\partial x} (\Gamma \sigma) \quad (4)$$

Equation (4) governs temperature fields in both solid and fluid regions. In the solid region, the convection terms are absent as velocities are identically zero. Because of the continuity requirement, the terms inside the third bracket on the left-hand side of Eq. (4) adds to zero.

Defining periodic fluxes as

$$\begin{aligned} \hat{J}_x &= \rho u \hat{\phi} - \Gamma \frac{\partial \hat{\phi}}{\partial x} \\ \hat{J}_y &= \rho v \hat{\phi} - \Gamma \frac{\partial \hat{\phi}}{\partial y} \end{aligned} \quad (5)$$

and substituting into Eq. (4) one gets

$$\frac{\partial \hat{J}_x}{\partial x} + \frac{\partial \hat{J}_y}{\partial y} = S - \rho u \sigma + \frac{\partial}{\partial x} (\Gamma \sigma) \quad (6)$$

In the above equation,  $S$  is the traditional source term and  $-\rho u \sigma$  and  $\partial(\Gamma \sigma)/\partial x$  are the first and second source terms as a result of periodically fully developed conditions. Therefore, when the conservation equation is written in terms of  $\hat{J}$ , it has two additional source terms. The first source term ( $-\rho u \sigma$ ) is included in the earlier investigations,<sup>3,4</sup> and the second source term  $\partial(\Gamma \sigma)/\partial x$  is not included. This omission of the second source term was the motivation for examining its importance in this work. Patankar and Prakash<sup>2</sup> considered the second source term for a case of infinitely conducting blockage. In this work, consideration is given to finitely conducting blockage. Also, the effects of heat transfer and flow parameters on the second source term are examined. The second source term will be zero only if the cause for the periodic flow is the periodic variation in shape of the channel wall. If conducting blockages are present in the flow path, then the second source term  $\partial(\Gamma \sigma)/\partial x$  is not zero, as the thermal conductivity of the fluid and solid are different. The thermal conductivity at the solid-fluid interface will be represented by the harmonic mean of the solid and fluid thermal conductivities. It should be noted that the second source term will be a nonzero quantity

only in control volumes that contain solid-fluid interface, which are normal to the streamwise direction. In the following section the implementation of the developed procedure is illustrated with the help of an example problem and its ramifications are discussed.

## Example

### Geometry

The geometry for the contrived example problem is shown in Fig. 1. Forced convective heat transfer in a rectangular channel with surface-mounted blocks on one of the walls is considered. The depth of the channel perpendicular to the plane of the paper is considered to be large enough to render the flow and heat transfer two-dimensional. The flow in the channel is assumed to be steady, incompressible, and laminar. The channel walls are insulated except at the surface of the blocks that coincide with the channel wall (the bottom surface). The bottom surfaces of the blocks are heated by subjecting them to uniform heat flux ( $q''$ ).

The cause for the periodically developed flow in this example problem is the presence of periodic blockage in the form of blocks. The objective of considering such an example problem is to be able to compare temperature fields obtained by solving the model equations for the developing flow (DF) with the one obtained by solving the model equations for the periodically developed flow (PDF), as discussed in the previous section. Far from the channel entrance the flow and heat transfer will be periodically developed. Hence, local heat flux and temperature distribution obtained by solving the periodically developed flow problem should be the same as the one obtained by solving the developing flow problem. Large numbers of modules are needed to achieve periodically fully developed flow and heat transfer. In this example problem, five modules were included and the fourth module was considered for comparison of DF and PDF solutions.

### Model Equations and Solution Technique

The model equations and associated boundary conditions for the DF problem are standard. As stated earlier, the main focus of this work is the handling of temperature field in the presence of conducting blockages. The treatment of momentum field can be found in Patankar.<sup>1</sup> The PDF model equations can be written as

1) Continuity:

$$\frac{\partial u}{\partial x} + \frac{\partial v}{\partial y} = 0 \quad (7)$$

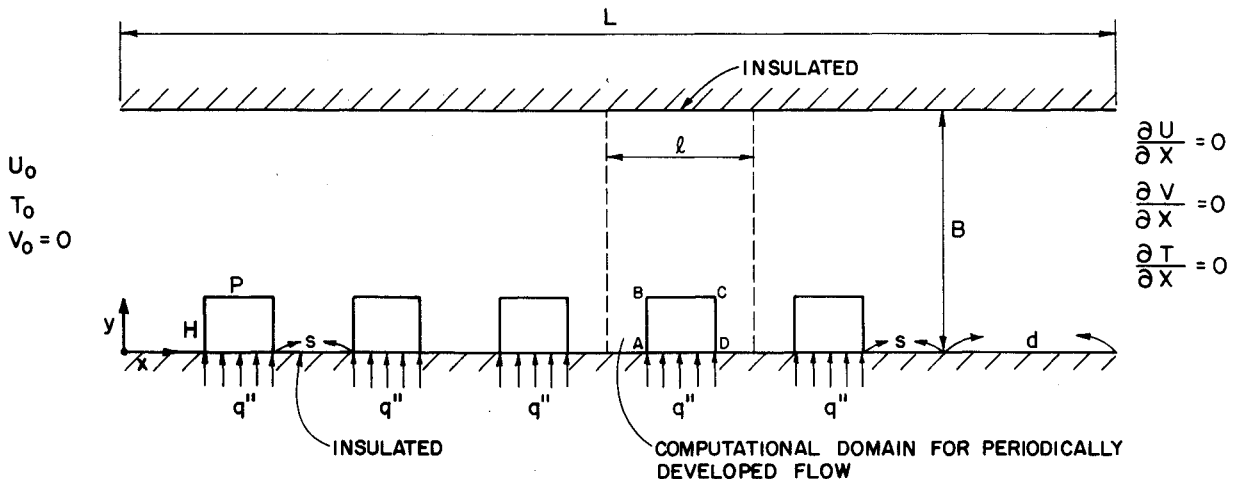


Fig. 1 An example: Developing flow and periodically fully developed flow in a channel.

2) *x* Momentum:

$$\rho \left( u \frac{\partial u}{\partial x} + v \frac{\partial u}{\partial y} \right) = \beta - \frac{\partial \hat{P}}{\partial x} + \frac{\partial}{\partial x} \left( \mu \frac{\partial u}{\partial x} \right) + \frac{\partial}{\partial y} \left( \mu \frac{\partial u}{\partial y} \right) \quad (8)$$

3) *y* Momentum:

$$\rho \left( u \frac{\partial v}{\partial x} + v \frac{\partial v}{\partial y} \right) = - \frac{\partial \hat{P}}{\partial y} + \frac{\partial}{\partial x} \left( \mu \frac{\partial v}{\partial x} \right) + \frac{\partial}{\partial y} \left( \mu \frac{\partial v}{\partial y} \right) \quad (9)$$

4) Energy:

$$\rho C_p \left( u \frac{\partial \hat{T}}{\partial x} + v \frac{\partial \hat{T}}{\partial y} \right) = \frac{\partial}{\partial x} \left( k^* \frac{\partial \hat{T}}{\partial x} \right) + \frac{\partial}{\partial y} \left( k^* \frac{\partial \hat{T}}{\partial y} \right) - \rho C_p \sigma u + \frac{\partial}{\partial x} (k^* \sigma) \quad (10)$$

where  $k^*$  is  $k_f$  in the fluid region,  $k_s$  in the solid region, and harmonic mean at the interface

$$\begin{aligned} p(x, y) &= -\beta x + \hat{P}(x, y) \\ \sigma &= [T(x + \ell, y) - T(x, y)]/\ell \\ &= \frac{q'' p}{\rho \bar{u} C_p B \ell} \end{aligned} \quad (11)$$

$\beta$  is the global pressure drop and  $\hat{P}(x, y)$  is the fluctuating component.  $\sigma$  is the global temperature rise and  $\hat{T}(x, y)$  is the local fluctuation. It should be noted that  $\beta$  is the input parameter and not  $Re$ . The corresponding Reynolds number can be calculated using the converged velocity field ( $Re = \rho \bar{u} B / \mu$ ). Thus, for every value of  $\beta$  there is a unique value of  $Re$ .

For the DF problem the fluid is assumed to enter the channel with a uniform velocity ( $U_0$ ) and temperature ( $T_0$ ). The exit of the channel is chosen so that it is far enough from the fifth block ( $d/B = 6$ ) so that the natural boundary conditions ( $\partial u / \partial x = \partial v / \partial x = \partial T / \partial x = 0$ ) could be imposed.

For the PDF problem, the  $u$  and  $v$  velocities repeat themselves from module to module, and it is stated as  $u(x, y) = u(x + \ell, y) = \dots$ , and  $v(x, y) = v(x + \ell, y) = \dots$ . However, only the fluctuating component of pressure and temperature repeats itself from module to module. Thus, boundary conditions are  $\hat{P}(x, y) = \hat{P}(x + \ell, y) = \hat{P}(x + 2\ell, y) = \dots$ , and  $\hat{T}(x, y) = \hat{T}(x + \ell, y) = \hat{T}(x + 2\ell, y) = \dots$ .

For both PDF and DF problems, the adiabatic condition ( $\partial T / \partial y = 0$ ) is imposed at the top wall ( $y = B$ ) and part of the bottom wall ( $y = 0$ ) that is not heated. The region of the bottom wall that coincides with the blocks is heated and this condition can be represented as

$$K_s \frac{\partial T}{\partial y} = K_s \frac{\partial \hat{T}}{\partial y} = q'' \quad (12)$$

A FORTRAN program was written to solve both PDF and DF problems using the SIMPLER algorithm.<sup>5</sup> Convection and diffusion terms were coupled by the power law. The set of discretization equations for the DF problem was solved by the line-by-line procedure by sweeping in one direction at a time. This technique is a combination of the Tri-Diagonal Matrix Algorithm (TDMA) and Gauss-Seidel procedure. The technique to solve the discretization equation for the PDF problem is the same as the one adapted for the DF problem, except that each line along the streamwise direction was solved by the Cyclic Tri-Diagonal Algorithm (CTDMA). For PDF

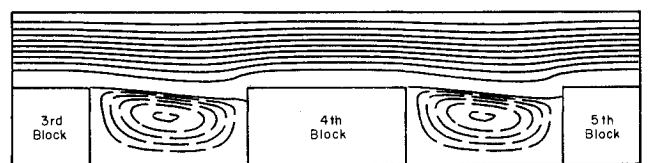
problems, the grid-independent solution was established when mass balance within each control volume and global heat balance were satisfied within 1%. Based on the grid independence studies, 149 grid lines were deployed in the streamwise direction and 39 grid lines in the cross-stream direction, to solve DF problem. The grid lines were nonuniformly spaced to capture steep gradients near the channel entrance and in the vicinity of solid-fluid interfaces. For the PDF problem, 28 nonuniform grid lines were deployed in the streamwise direction and 39 nonuniform spaced grid lines in the cross-stream direction. Convergence for each run was declared when the maximum residue of each equation was less than  $10^{-5}$ .

## Results and Discussion

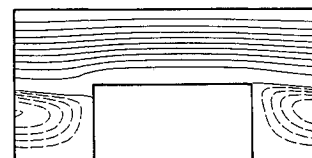
The governing geometric parameters of this example problem are the channel-length-to-height ratio ( $L/B$ ), ratio of the block length to the channel height ( $p/B$ ), ratio of the block height to the channel height ( $H/B$ ), and the ratio of the spacing between the blocks to the channel height ( $S/B$ ). In this investigation calculations were made for standard values of geometric parameters ( $L/B = 16$ ,  $p/B = 1$ ,  $H/B = 0.25$ , and  $S/B = 1$ ). The governing flow and heat-transfer parameters are Reynolds numbers ( $Re$ ), Prandtl numbers ( $Pr$ ), and the ratio of the thermal conductivity of the solid to fluid ( $K = k_s/k_f$ ). For the purpose of illustration of the procedure and to study the impact of the second source term in the energy equation, calculations were made for  $Re = 4, 40$ , and  $372$ ;  $Pr = 0.7$ , and  $k_s/k_f = 10, 100$ , and  $500$ . In addition to the standard geometric parameters, calculations were made for  $H/B = 0.5$  and  $P/S = 2$ .

Figure 2 shows the comparison of streamlines for the DF and PDF channels. In Fig. 2a the computational domain extends from the rear half of the third block to the front half of the fifth block. It is evident in Fig. 2a that the streamlines are almost identical in each of the modules. The left recirculation pocket (between the third and fourth blocks) has a minimum value of  $\Psi = -0.05103$  and the right recirculation pocket (between the fourth and fifth blocks) has a minimum value of  $\Psi = -0.05101$ . Hence, we can conclude that the flow is almost periodically fully developed. The streamline distribution for the PDF problem is shown in Fig. 2b. The minimum value of  $\Psi$  for the PDF solution is equal to  $-0.0508$ . The value of  $\Psi$  and the shape of streamlines for PDF and DF problems compare well and this provides a sound basis for examining the temperature field.

The PDF temperature field should agree with the DF temperature field far from the channel entrance. Thus, to examine the importance of the second source term the local heat flux and temperature distributions obtained by solving DF and PDF problems for the fourth block are compared in Fig. 3.



a) Streamlines for DF;  $(\Psi_{\min})_{\text{left}} = -0.05103$ ,  $(\Psi_{\min})_{\text{right}} = -0.05101$



b) Streamlines for PDF;  $\Psi_{\min} = -0.0508$

Fig. 2 Comparison of streamlines for DF and PDF problems;  $Re = 40$ ,  $H/B = 0.5$ ,  $P/S = 1$  ( $\Delta\Psi = 0.1$  in mainstream region,  $\Delta\Psi = 0.01$  in recirculation region).

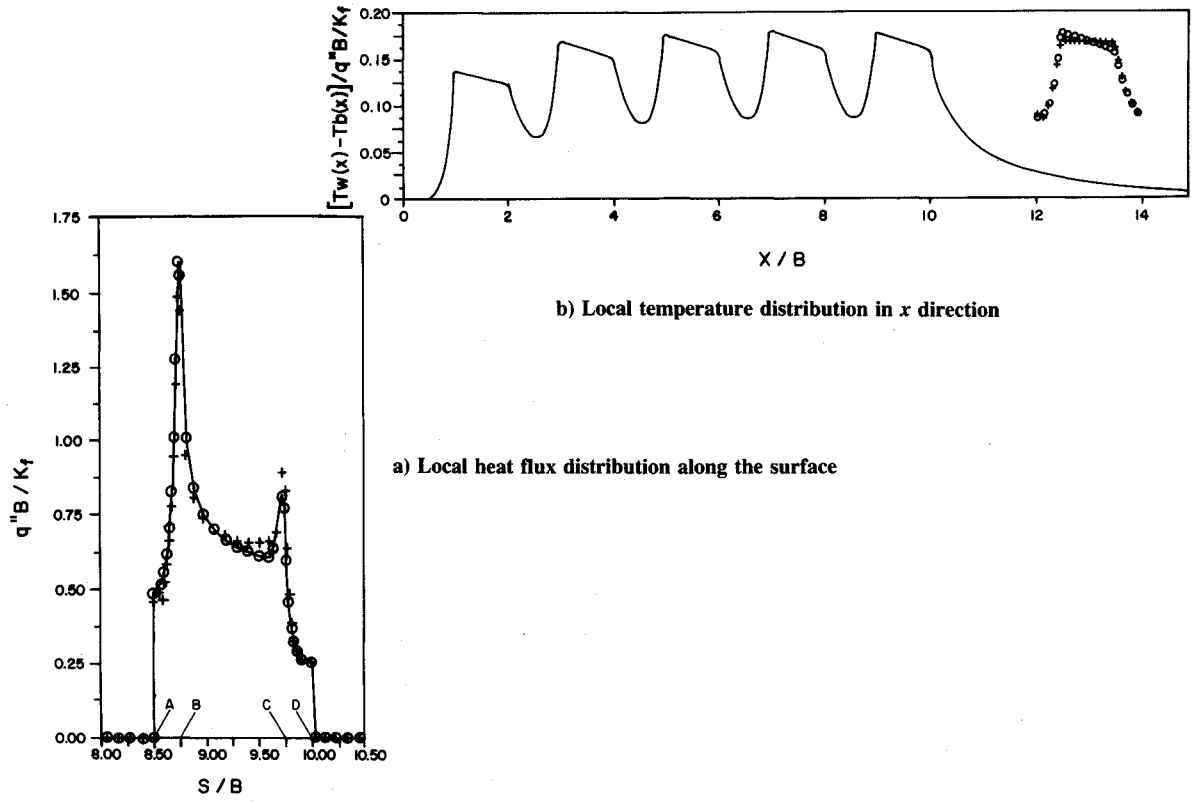


Fig. 3 Comparison of DF and PDF solutions:  $Re = 40$ ,  $K = 100$ ,  $Pr = 0.7$ ; —, DF;  $\circ$ , PDF with second source term; +, PDF without second source term.

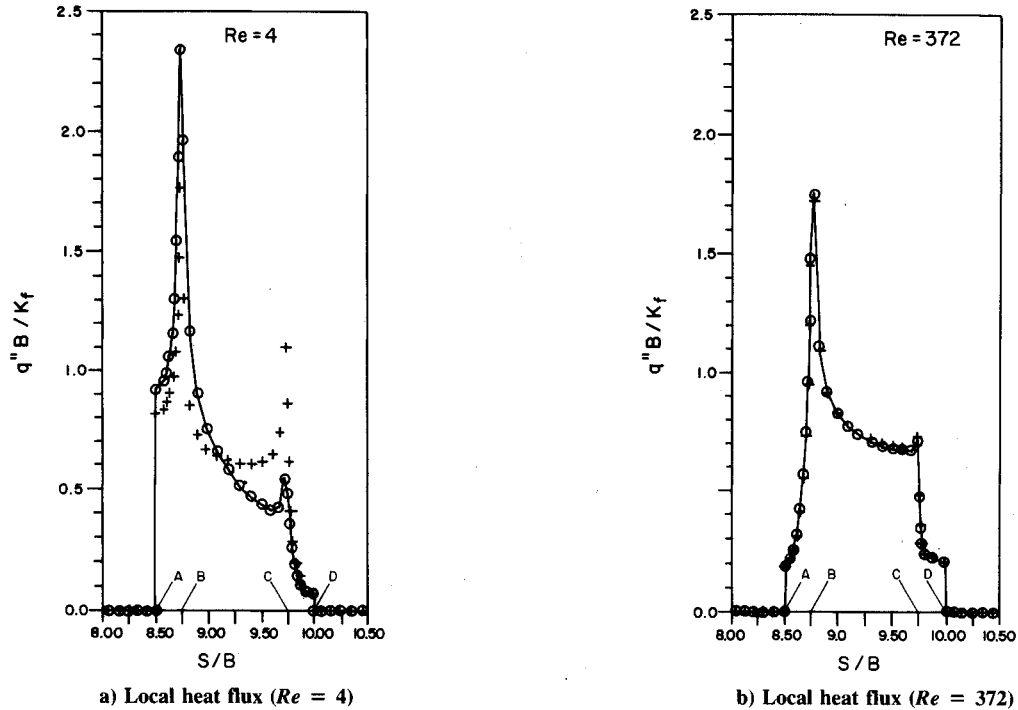


Fig. 4 Effect of  $Re$  on heat flux distribution:  $K = 100$ ,  $Pr = 0.7$ ; —, DF;  $\circ$ , PDF with second source term; +, PDF without second source term.

The relationship between the local heat flux and temperature can be stated as

$$q''_y = \pm K_f \frac{\partial T}{\partial y} = \pm K_f \frac{\partial \hat{T}}{\partial y} \quad (13)$$

$$q''_x = \pm K_f \frac{\partial T}{\partial x} = \pm K_f \left( \sigma + \frac{\partial \hat{T}}{\partial x} \right) = \pm K_f (\sigma + \hat{q}''_x) \quad (14)$$

$$T_w(x) - T_b(x) = \hat{T}_w(x) - \hat{T}_b(x) \quad (15)$$

It is evident from Figs. 3a that without the second source term the local heat flux distribution obtained by solving the PDF problem is significantly different from the solution obtained by solving the DF problem. Without the second source term the PDF solution underpredicts heat flux along the front and upstream part of the top surface of the block. On the

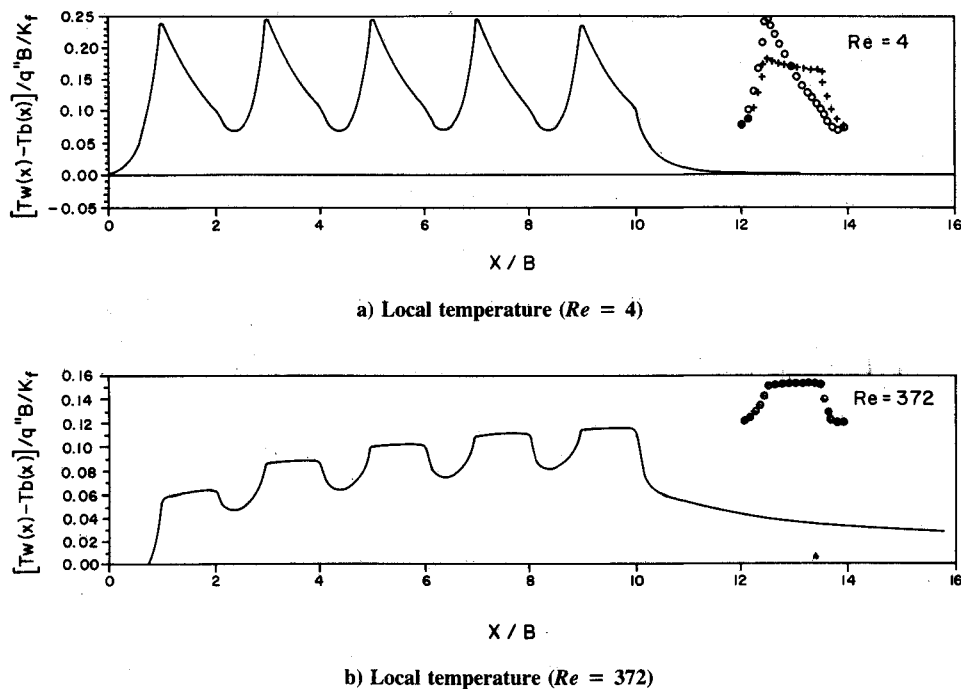


Fig. 5 Effect of  $Re$  on temperature distribution:  $K = 100$ ,  $Pr = 0.7$ ; —, DF;  $\circ$ , PDF with second source term; +, PDF without second source term.

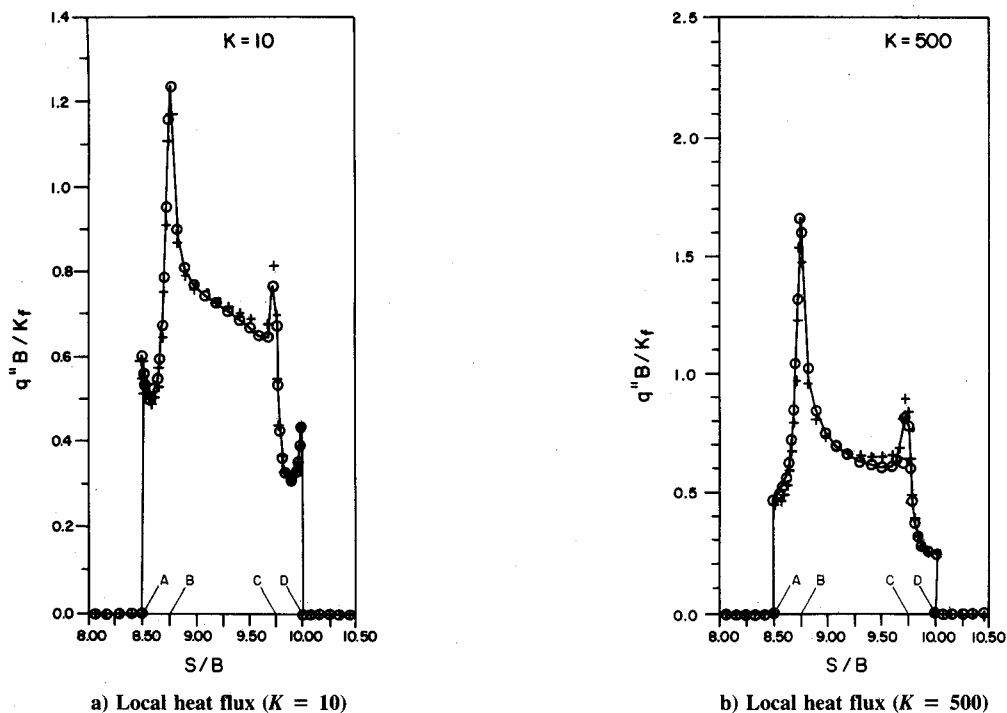


Fig. 6 Effect of thermal conductivity ratio on heat flux:  $Re = 40$ ,  $Pr = 0.7$ ; —, DF;  $\circ$ , PDF with second source term; +, PDF without second source term.

other hand, along the downstream part of the top surface and the rear surface of the block, the heat flux is overpredicted. It should be noted that the local temperature referred to in Fig. 3 is actually the difference between the wall temperature and the bulk temperature of the flow. By including the second source term in the energy equation, the PDF solution agrees very well with the DF solution, thus highlighting the importance of the second source term. Incorrectly predicted local distributions of temperature and heat flux will eventually lead to incorrect overall heat-transfer characteristics of the channel. However, no special consideration is given to the discussion of local or average Nusselt number, as the main focus

of this paper is to investigate the importance of the second source term.

Figures 4 and 5 display the effect of Reynolds number on the second source term. From Fig. 4a it is clear that the local heat flux distribution without the second source term for the PDF solution is very different from the DF solution. As  $Re$  increases, the effect of the second source term diminishes. It can be seen in Fig. 4b that for  $Re = 372$  the impact of the second source term is minor. The same behavior is observed with the help of local temperature distributions (Figs. 5a and 5b). This behavior is expected as  $\sigma$  is inversely proportional to the average flow velocity ( $\bar{u}$ ), which in turn is proportional

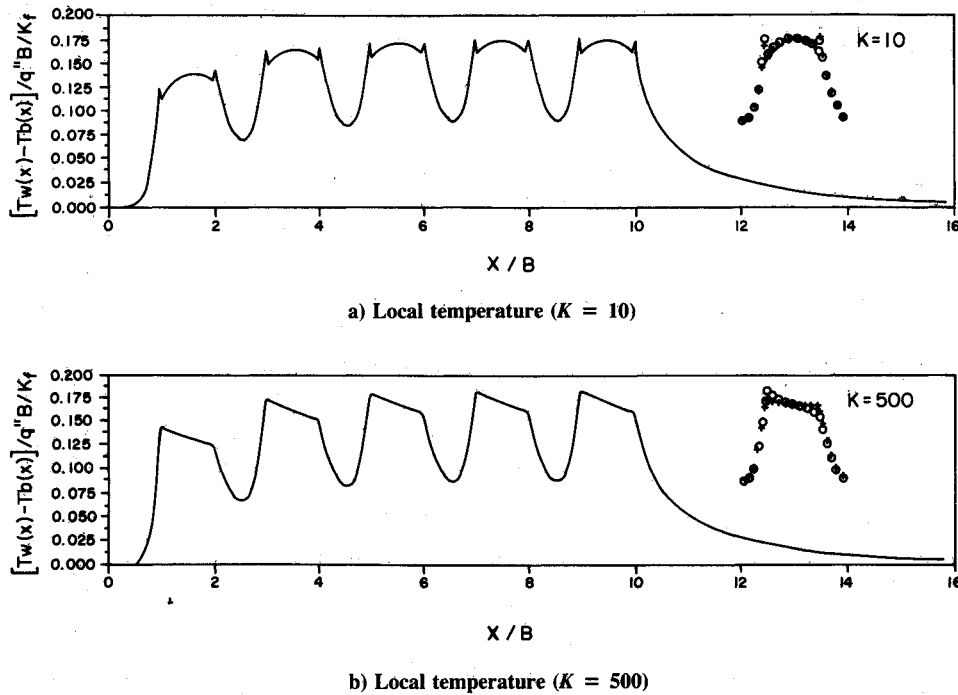


Fig. 7 Effect of thermal conductivity ratio on temperature distribution:  $Re = 40$ ,  $Pr = 0.7$ ; —, DF;  $\circ$ , PDF with second source term; +, PDF without second source term.

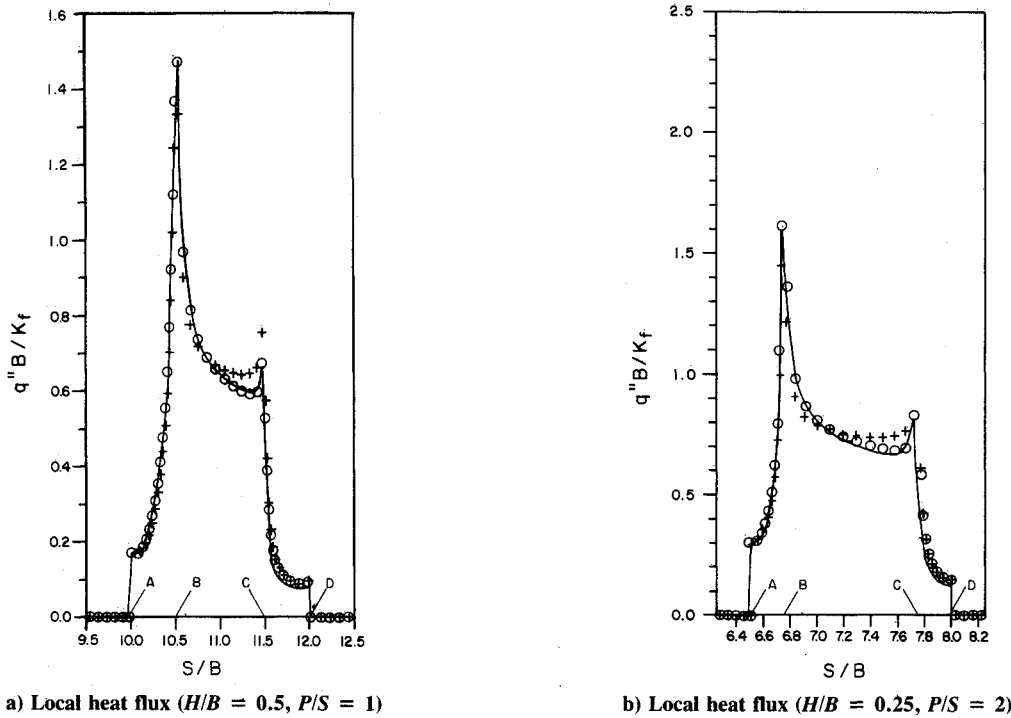


Fig. 8 Local heat flux distribution:  $Re = 40$ ,  $Pr = 0.7$ ,  $K = 100$ ; —, DF;  $\circ$ , PDF with second source term; +, PDF without second source term.

to the  $Re$ . For the same reason, any factor contributing toward increase in  $\sigma$  would strengthen the second source term. From Eqs. (10) and (11) it is clear that the second source term inversely varies as the Prandtl number ( $Pr$ ). At higher values of  $Re$  ( $Re = 372$ ) the DF and PDF temperature distribution do not match well (Fig. 5b), the reason being higher  $Re$  values require longer entrance region, thus warranting the inclusion of additional blocks. Further addition of blocks requires prohibitively large amounts of CPU time which is not available to this investigation.

The effect of  $K$  on the second source term is shown in Figs. 6 and 7. At lower values of  $K$  ( $K = 10$ ) the influence of the

second source term is less and when  $K$  value is increased to 500, the influence of the second source term is greater. This behavior is echoed by both the local heat flux (Figs. 6a and 6b) and the local temperature distributions (Figs. 7a and 7b). It is to be noted that the increase in  $K$  results in increases in the strength of the second source term.

The effect of geometric parameters on the second source term was studied by varying  $H/B$  and  $P/S$  one at a time while keeping the rest of the geometric parameters at standard values as stated earlier. The local heat flux distribution for  $H/B = 0.5$ ,  $P/S = 1$  and  $H/B = 0.25$ ,  $P/S = 2$  is shown in Figs. 8a and 8b, respectively. Similarly, the local temperature dis-

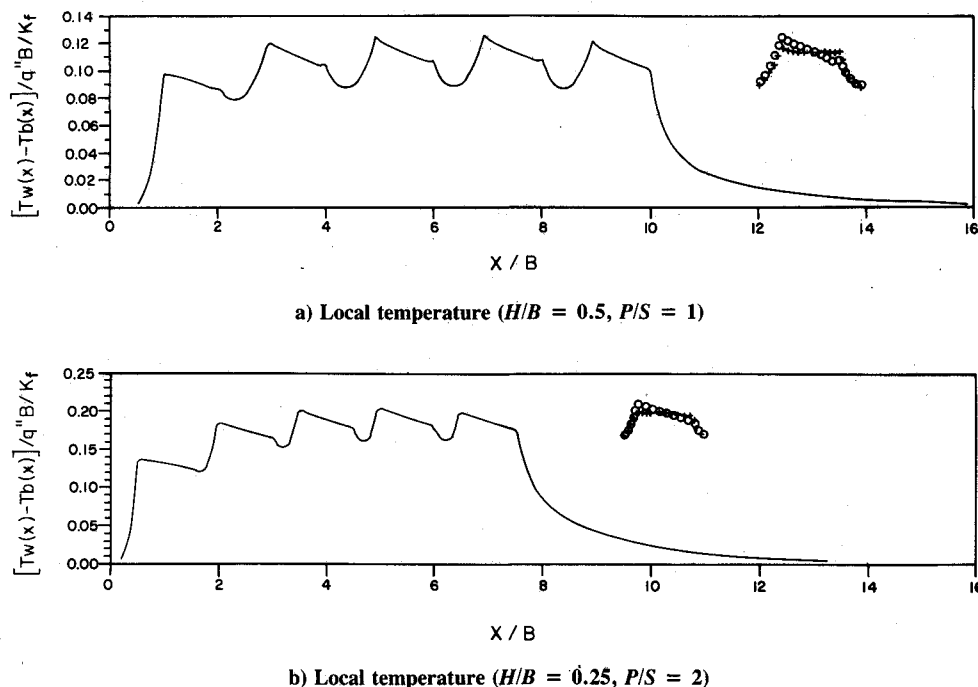


Fig. 9 Local temperature distribution:  $Re = 40$ ,  $Pr = 0.7$ ,  $K = 100$ ; —, DF;  $\circ$ , PDF with second source term; +, PDF without second source term.

tribution for  $H/B = 0.5$ ,  $P/S = 1$  and  $H/B = 0.25$ ,  $P/S = 2$  is shown in Figs. 9a and 9b, respectively. From these figures it is evident that the second source term will continue to affect the local temperature and heat flux distributions when the geometric parameters are altered. In this investigation only two variations in geometric parameters ( $H/B = 0.25$ ,  $0.5$  and  $P/S = 1, 2$ ) were examined to highlight the importance of the second source term.

### Summary

The importance of the second source term  $\partial(K\sigma)/\partial x$  in the energy equation is examined by solving a contrived example problem. Generally, heat flux at the upstream of the block is underpredicted and heat flux at the downstream surface of the block is overpredicted when the second source term is not considered. Thus inclusion of the second source term results in prediction of the correct temperature field. The impact of the second source term is found to increase with an increase in the thermal conductivity ratio of the solid to fluid ( $K$ ) and decrease with increase in  $Re$  and  $Pr$ . In conclusion, any parameter that would increase  $K\sigma$  will strengthen the second source term warranting its inclusion in the energy equation.

### Acknowledgments

This work was supported in part by the Texas A&M University Engineering Excellence Fund. Time on NEC-SX-2 was made available through a grant from the Houston Area Research Center (HARC).

### References

- Patankar, S. V., Liu, C. H., and Sparrow, E. M., "Fully Developed Flow and Heat Transfer in Ducts Heating Streamwise-Periodic Variations of Cross-Sectional Area," *ASME Journal of Heat Transfer*, Vol. 99, 1977, pp. 180–186.
- Patankar, S. V., and Prakash, C., "An Analysis of the Effect of Plate Thickness on Laminar Flow and Heat Transfer in Interrupted-Plate Passages," *International Journal of Heat and Mass Transfer*, Vol. 24, 1981, pp. 1801–1810.
- Webb, B. W., and Ramadhyani, S., "Conjugate Heat Transfer in Channels with Staggered Ribs," *International Journal of Heat and Mass Transfer*, Vol. 28, 1985, pp. 1679–1687.
- Asako, Y., and Faghri, M., "Three-Dimensional Heat Transfer and Fluid Flow Analysis of Arrays of Square Blocks Encountered in Electronic Equipment," *Numerical Heat Transfer*, Vol. 13, 1988, pp. 481–498.
- Patankar, S. V., *Numerical Heat Transfer and Fluid Flow*, McGraw-Hill, New York, 1980.